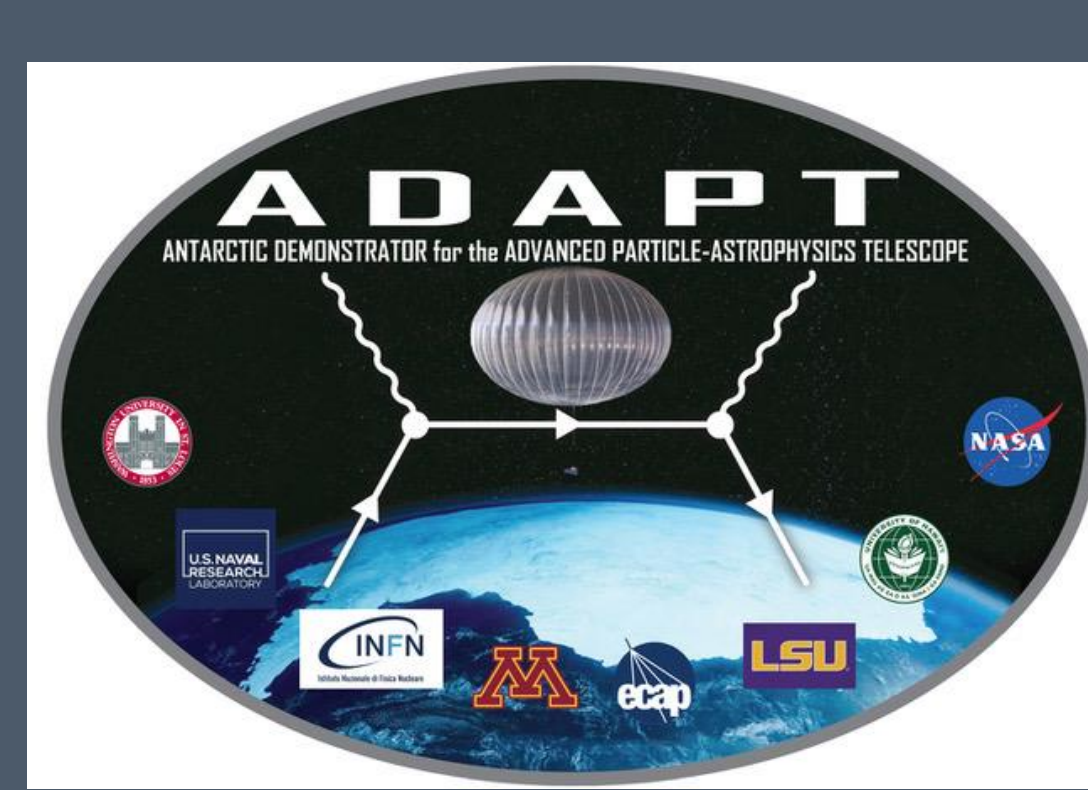


The Advanced Particle-astrophysics Telescope: Simulation of the Instrument Performance for Gamma-Ray Detection

Wenlei Chen¹ and James H. Buckley² on behalf of the APT Collaboration*

1. School of Physics and Astronomy, University of Minnesota, Minneapolis, MN 55455, USA
2. Washington University in St. Louis, Dept. Physics, One Brookings Drive, Saint Louis, MO 63130, USA



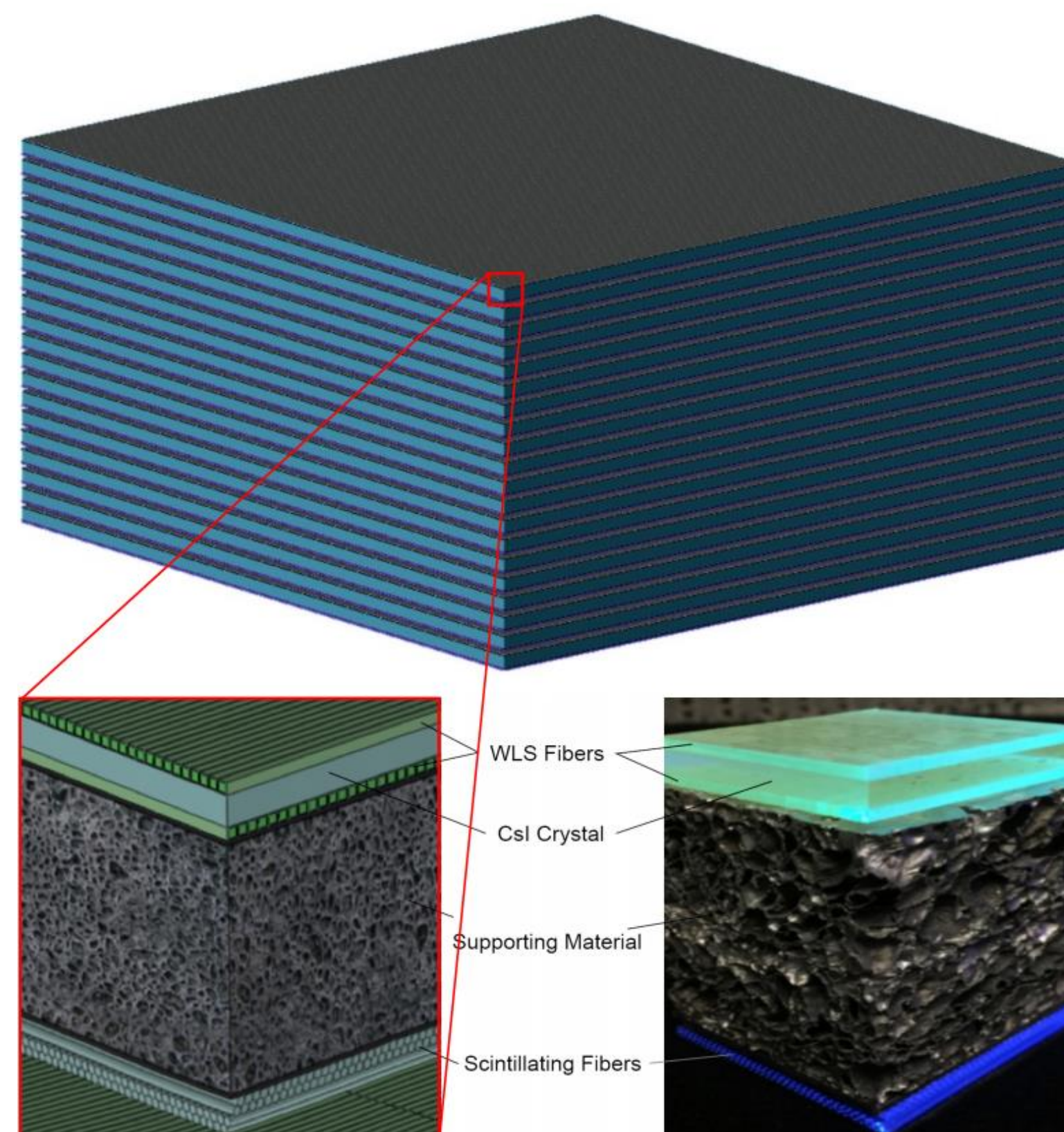
INTRODUCTION

The Advanced Particle-astrophysics Telescope (APT) and the Antarctic Demonstrator for APT (ADAPT)

- The Advanced Particle-astrophysics Telescope (APT) is a high-energy gamma-ray and cosmic-ray mission concept. The instrument design is aimed at maximizing effective area and field of view for MeV-TeV gamma-ray and cosmic-ray measurements. Considering the limit payload mass and instrument cost, we propose a detector design based on 3-meter scintillating fibers read out by Silicon photomultipliers (SiPMs). The APT detector includes a multiple-layer tracker composed of scintillating fibers and an imaging calorimeter composed of thin layers of sodium-doped CsI (CsI:Na) scintillators and wavelength-shifting (WLS) fibers. The CsI:Na crystals are coupled to crossed planes of wavelength shifting fibers to localize energy deposition to ~mm accuracy. With about half of the number of electronic readout channels of the Fermi Gamma-ray Space Telescope (FGST) Large Area Detector (LAT) and a relatively shallow (< 6 radiation length) calorimeter, our simulations show that the critical performance requirements can be met within a reasonable payload mass for available launch vehicles.
- The Antarctic Demonstrator for APT (ADAPT) is a balloon experiment using a small portion ~1% of the APT detector. The ADAPT experiment will demonstrate the potential of our instrument concept and test our gamma-ray and cosmic-ray reconstruction algorithms.
- The major scientific goals of the APT experiment include fast, all-sky, and large effective area detection and localization of gamma-ray bursts (GRBs) and other gamma-ray transients such as gravitational wave counterparts and searches for thermal dark-matter particles over the entire natural range of masses and total annihilation cross section.

Detector Construction

- The baseline APT detector has a uniform, multi-layer structure. Each layer of the detector consists of an array of cylindrical, multi-clad scintillating fibers that serve as a tracker, supporting materials/transition radiator, a thin CsI:Na crystal layer coupled to a top (X) and bottom (Y) plane of 2 mm square WLS fiber that behaves as both a pair-converter and a calorimeter. The baseline instrument is composed of a 3m×3m active area with 20-40 detector layers, limited by the size of the fairings (and lift capacity) of existing launch vehicles.
- The current design of the ADAPT includes four layers of scintillating-fiber-tracker and imaging-CsI-calorimeter modules of 45mm×45mm. We will also place photo detectors on the edges of the CsI:Na crystal to collect scintillation light that is not piped into the optical fibers. On the bottom of the 4-layer imaging detector, there will be 4 additional layers of CsI:Na calorimeter without wavelength-shifting fibers to increase the radiation length of the detector for GeV gamma-ray observations.



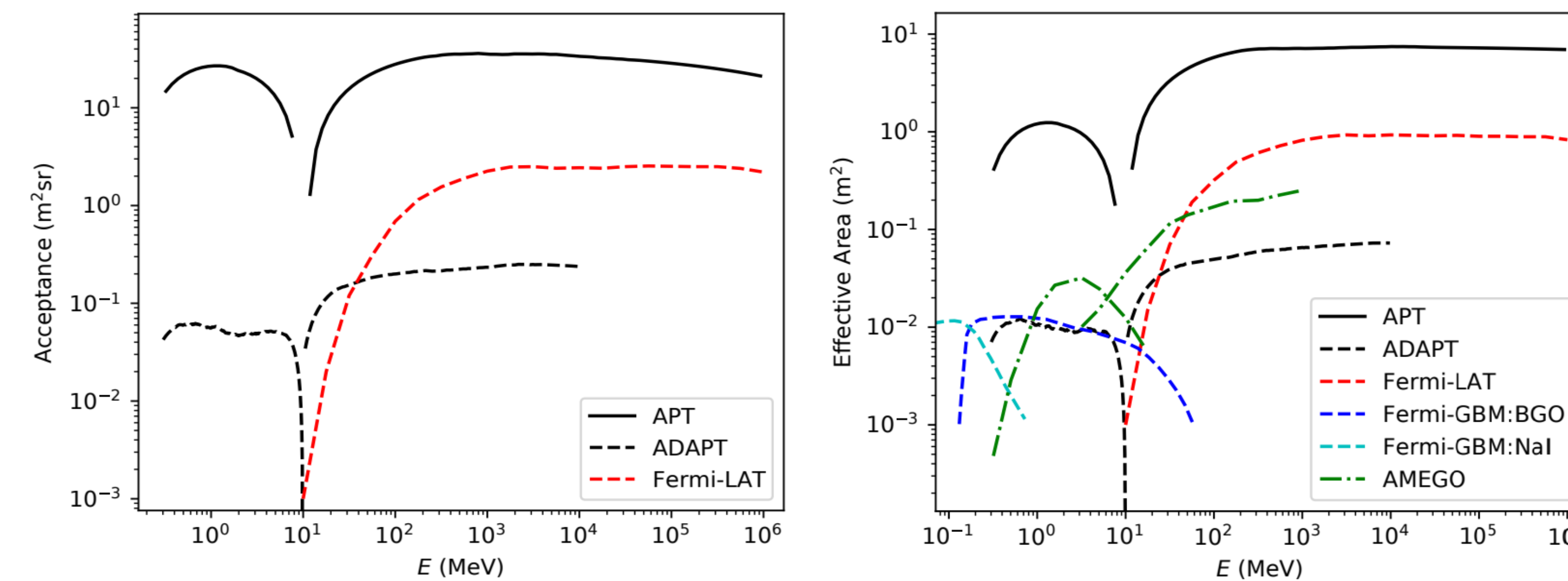
Top: the APT main detector. Bottom: one layer of the APT detector prototype. (Left) solid model of the detector geometry. Right: a small cross section constructed out of actual scintillating fibers and an aluminum honeycomb for demonstration.

SIMULATION AND RECONSTRUCTION

- We developed a simulation package called APTsoft that includes scripts to generate geometry configuration files, Geant4 simulation code to simulate gamma-ray and cosmic-ray interactions with the detector, optical simulation code of light collection and electronics detection, and gamma- and cosmic-ray event analysis tools to calculate instrument performance. The specifications of the detector response for the simulations are derived from measured performance parameters from prototype tracker fibers and a prototype of the CsI detector.
- At energies above 30 MeV, pair production is the dominant photon interaction in most materials, by which an electron-positron pair is created as the cosmic gamma-ray interacts in the electric fields of atoms in the detector. At lower energies (< 10 MeV), incident gamma-rays experience multiple Compton scatterings. The APT instrument will function both as a pair telescope for 30 MeV to 1 TeV gamma-rays and as a Compton telescope with excellent sensitivity down to ~0.3 MeV.

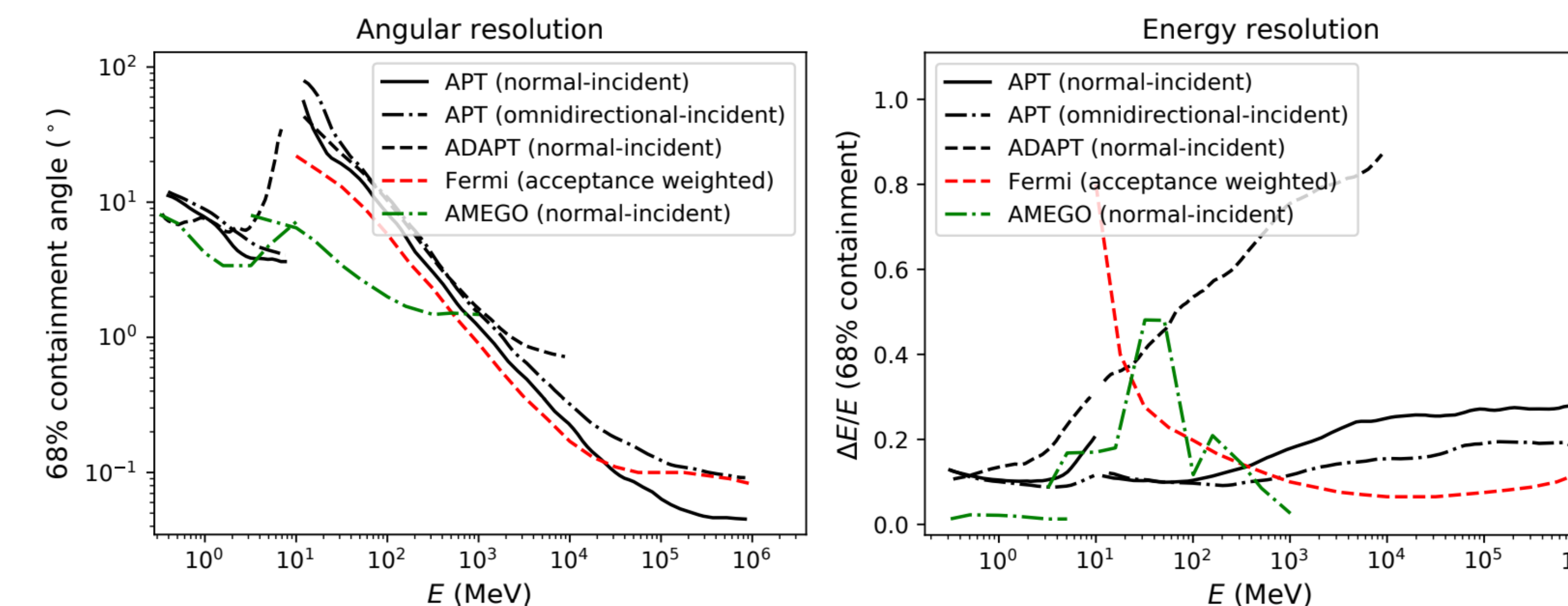
PERFORMANCE

Geometric Factor and Effective Area



Acceptance/geometry factor (left) and normal-incident effective area (right) versus energy. The lower energy solid black curves denote APT Compton reconstruction and the higher denote APT pair reconstruction. Dashed red and dash-dotted green curves are for Fermi P8R2_SOURCE_V6 events and AMEGO, respectively. Dashed blue and cyan curves show the Fermi-GBM effective area for the BGO and NaI detectors, respectively.

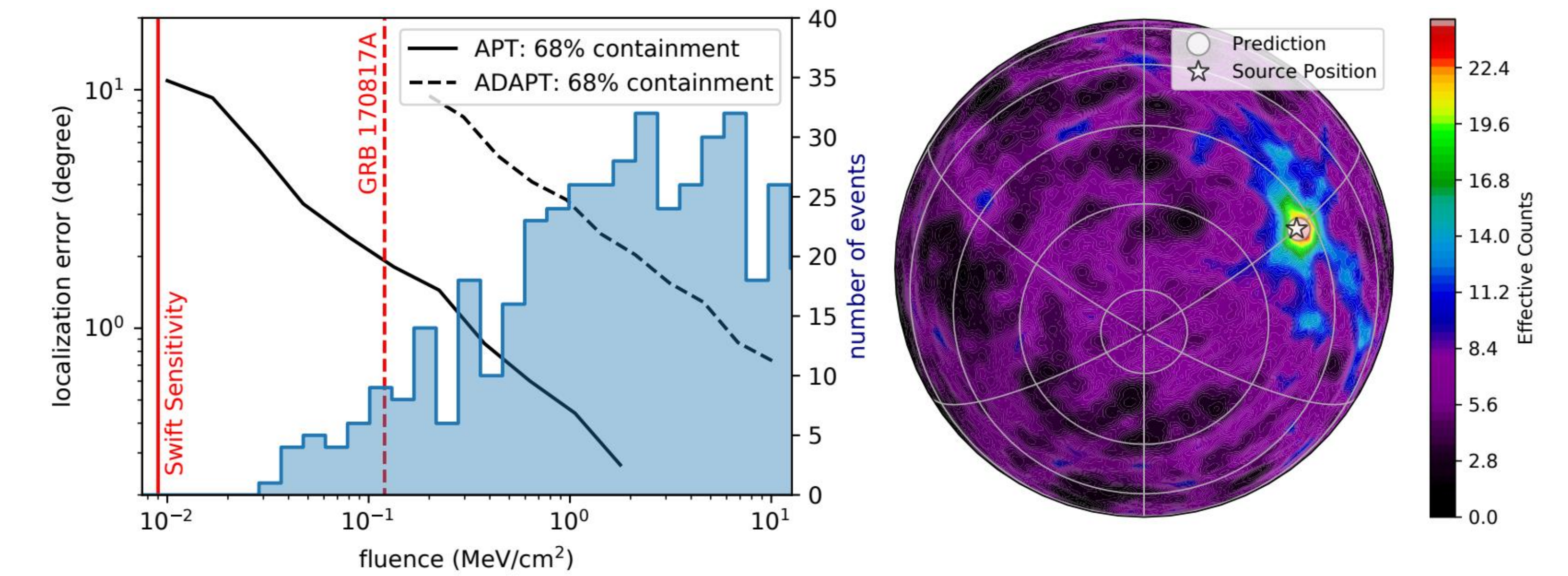
Angular and Energy Resolution



Angular resolution (left) and energy resolution (right) as shown by the 68% containment versus energy. Solid and dash-dotted black curves are for APT with normal- and omnidirectional-incident events. Dashed black, red, and dash-dotted green curves are for ADAPT, Fermi P8R2_SOURCE_V6 events, and AMEGO, respectively.

Gamma-Ray Burst (GRB) Localization

- The localization of a GRB is conducted by calculating the centroid of the reconstructed sky map, i.e., the distribution of Compton rings. We simulated a number of GRBs with spectral energy distribution based on the Band's function for a range of fluence values from multiple incident directions with inclination angles > 45° from the detector's X-Y plane.
- As we can see, APT has degree-level accuracy of localizing faint GRBs. For bright GRBs with fluence > 1 MeV/cm², the APT and ADAPT have localization accuracy at sub-degree and degree levels.

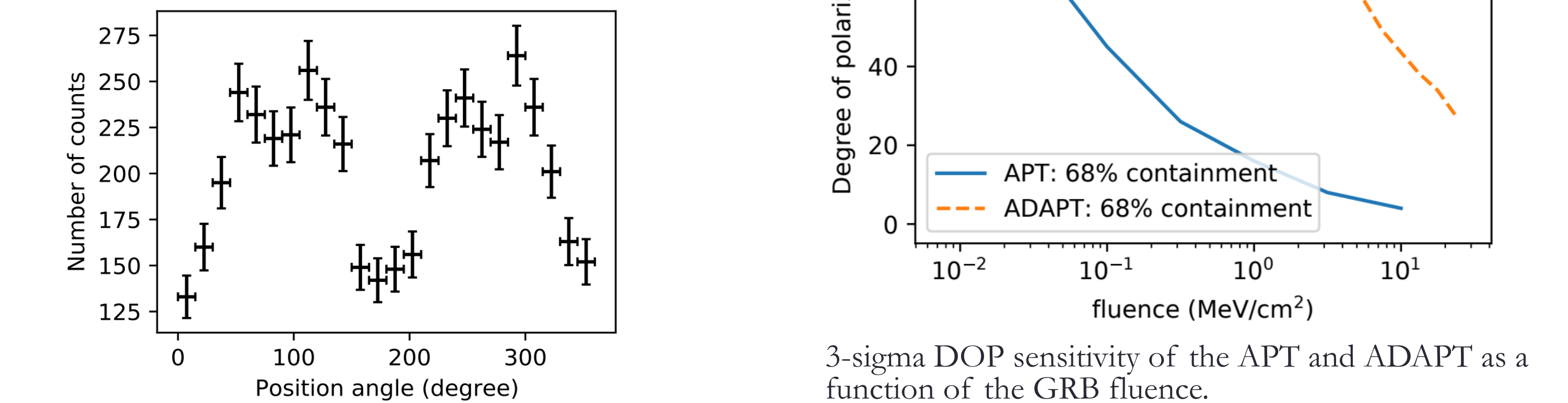


Left: Error in reconstructed direction of a Band-spectrum GRB versus fluence. The red solid and dashed line shows the estimated fluence of Swift sensitivity limit and GRB170817A/ GW170817 event in the APT energy range. Histogram shows the count rate of GRBs from the first Fermi-GBM catalog in the energy range from 10 keV to 1 MeV. Right: An example Compton sky map of a 1 MeV/cm² GRB detected by the ADAPT.

GRB Polarization

- The large effective area and intrinsic sensitivity of Compton scattering to polarization makes APT a very powerful polarimeter for measuring both the degree of polarization and polarization angles for GRBs at MeV energies. We estimate the significance of the polarization measurement by evaluating the significance of getting a maximum counts value at a position angle perpendicular to the polarization vector where the count rate is minimized. For a 3-sigma detection significance, we calculated the degree-of-polarization (DOP) sensitivity for GRBs with a power-law spectrum as a function of the GRB fluence. As we can see, polarization of typical long GRBs with fluence of 1 MeV/cm² can be significantly detected by the APT with DOP down to ~10%.

Distribution of scattered gamma-rays detected by the ADAPT as a function of azimuthal position angle for an example of linear polarized GRB (along 0-180°) with fluence of 1 MeV/cm².



3-sigma DOP sensitivity of the APT and ADAPT as a function of the GRB fluence.

* S. Al Nussir¹, C. Altomare², R.G. Bose³, W.R. Binns⁴, D. Braun⁵, J.H. Buckley⁶, J.D. Buhler⁷, E. Burns⁸, R.D. Chamberlain⁹, W. Chen⁶, M.L. Cherry¹, M. Errando³, S. Funk⁶, F. Giordano¹⁰, J. Hoffman¹¹, Z. Hughes¹², D. Huth¹³, P.L. Kelly¹⁴, J.F. Krizmanic^{15,16}, M. Kuwahara¹⁷, F. Liccioli¹⁸, G. Liu¹², M.N. Mazziotta¹⁹, J.W. Mitchell²⁰, G.A. de Nolfo²¹, R. Paoletti²², R. Pillera²³, B.F. Rauch²⁴, D. Senni²⁵, G. Simburger²⁶, M. Sudwar²⁷, G.S. Varner²⁸, L. Di Venere²⁹, E. Wulf³⁰, A. Zink³¹, W.V. Zob³²
¹Department of Physics and Astronomy, Louisiana State University, Baton Rouge, Louisiana 70803, USA, ²Istituto Nazionale di Fisica Nucleare, Sezione di Bari, I-70126 Bari, Italy, ³Department of Physics and McDonnell Center for the Space Sciences, Washington University, St. Louis, MO 63130, USA, ⁴Department of Computer Science & Engineering, Washington University, St. Louis, MO 63130-4899, USA, ⁵Department of Physics and Astronomy, University of Minnesota, Minneapolis, MN 55455, USA, ⁶Friedrich-Alexander-Universität Erlangen-Nürnberg, Erlangen Centre for Astroparticle Physics, D-91058 Erlangen, Germany, ⁷Dipartimento di Fisica "M. Merlin" dell'Università e del Politecnico di Bari, I-70126 Bari, Italy, ⁸Center for Space Sciences and Technology, University of Maryland Baltimore County, Baltimore, Maryland 21250, USA, ⁹Astroparticle Physics Laboratory, NASA/GSFC, Greenbelt, Maryland 20771, USA, ¹⁰Center for Research and Exploration in Space Sciences and Technology, NASA/GSFC, Greenbelt, Maryland 20771, USA, ¹¹Department of Engineering, University of Hawaii at Manoa, Honolulu, HI 96822, USA, ¹²Department of Physics and Astronomy, University of Hawaii at Manoa, Honolulu, HI 96822, USA, ¹³Heliophysics Physics Laboratory, NASA/GSFC, Greenbelt, Maryland 20771, USA, ¹⁴Università di Siena and INFN Pisa, I-53100 Siena, Italy, ¹⁵Politecnico di Bari, Department of Mechanics, Mathematics and Management, via Orabona, 4, I-70125 Bari, Italy, ¹⁶Naval Research Laboratory, Washington, DC 20375, USA.